ISSN No:-2456-2165

Numerical Investigation on the Performance of Various Wall Functions on Heat Transfer Enhancement

Saleh Etag[1], Nabil Elsharif[1]
University of Benghazi
Mechanical Engineering Department, Libya

Abstract:- The present work focus on the study of the wall functions as a tool to capture the heat transfer rate in the near wall region. Various wall functions were tested such as: equilibrium wall function, enhanced wall function, scalable wall function and standard wall function. A vertical pipe case was tested and investigated thoroughly to ascertain the applicability of each wall function, the governing equations were solved with boundary conditions, finite volume method was used to solve the continuity equation, momentum equation and the energy equation. It was found that enhanced wall function showed a better behavior for capturing the heat performance in the vicinity of the wall.

I. INTRODUCTION

The treatment of wall boundaries requires particular attention in turbulence modelling. The reason is that in the vicinity of the wall the turbulent shear stress falls rapidly within the buffer layer as the wall is approached, thus, there is a thin viscous sublayer near the wall where only the viscous stress is important. It is the presence of this viscous sublayer which is responsible for the extremely sharp gradients of mean and turbulent flow variables near the wall.

The resolution of the viscosity-dominated region can be achieved if a fine numerical grid is employed. This is the so-called 'low-Reynolds-number' approach. The fine grid is needed to capture accurately the gradients of the mean and turbulent quantities, and their variations, which can be substantial in the vicinity of the wall. As the bulk Reynolds number of the flow becomes higher the grid problem becomes more severe, because the size of the viscous sublayer becomes smaller. As a result, the grid must be strongly compressed towards the wall and the spacing in the turbulent region may need to be reduced near the edge of the buffer layer also, in order to match the sublayer grid. In the case of fluids with a Prandtl number greater than unity the thermal viscous sublayer is thinner than the hydrodynamic one, and consequently the low-Reynolds-number calculation in this case is then more expensive as further grid compression should be made to ensure adequate resolution of the thermal sublayer. Although there is a rapid growth in computer technology and improvements in numerical methods, there remains a great problem in resolving industrial 3D flows, where the accurate low-Reynolds-number resolution of the near-wall sublayer with structured-grid schemes can be responsible for about 90% of all computing costs.

As one might expect, some attempts have been made to eliminate, or at least substantially reduce, the above problem and make the computations much cheaper. Many of these attempts were made near the beginning of the CFD, when computers were slow and the cost of computing simple engineering problems was extremely severe. In the meanwhile, Wall Functions were introduced which provide an alternative to prescribing the viscous wall boundary conditions. They bridge the gap between the viscous sub layer and the fully turbulent region. However, most existing wall functions are based on the prescription of a velocity which varies as the logarithm of distance from the wall: a variation which is valid only under local-equilibrium flow conditions.

Understandably, these wall functions achieve a low accuracy in non-equilibrium conditions. It goes without saying that complex industrial applications include flows with separation and/or reattachment regions and often include flows where buoyant effects are significant. All the above-mentioned flows depart from a state of local equilibrium; it is therefore inappropriate to apply such basic wall functions to these types of flows. For example, in Craft et al[1] it is noted that these limitations were recognised from the earliest days of turbulent flow CFD.

Spalding [2] developed an elaborate set of formulae that aimed to account for modifications to the usual log-law formulae caused by pressure gradients and mass transfer through the wall, as well as circumstances where the wall function only had to account for a portion of the sublayer. Patankar and Spalding[3] developed similar, if somewhat less general, wall functions again incorporating effects of mass transfer and pressure gradient. This work was soon followed by a parallel treatment by Wolfshtein[4] whose analysis was the first to incorporate the effects of high external levels of turbulence energy convected or diffused towards the wall.

However the above schemes, developed in the late 1960's, were not widely used but instead were replaced in CFD software by the conventional logarithmic laws for velocity and temperature; the only improvement to the original logarithmic law of Prandtl being that the square root of the turbulence energy has been used instead of friction velocity,. Moreover, even for industrial type applications it was recognised that relatively advanced wall functions did not give clearly superior results to a simple log-law formulation. There were evidently some important physical effects missing even from the elaborate forms and, in any event, none of the schemes included the effects of buoyancy.

There continuous attempts at refining the wall function analysis was first by Chieng and Launder[5] who have developed a wall function which is simply based on the variation of turbulent kinetic energy and turbulent shear stress across the fully turbulent region of the near-wall cell, another attempt by Johnson & Launder[6] attempted to takes into consideration for changes of the viscous sublayer thickness in their proposed wall function. Amano[7] resolved the equation for the dissipation rate of the turbulent energy across the near-wall cell using cell-averaged production and destruction terms. later, Amano[8] developed his approach by considering a three-zone wall function, he made different prescriptions for the turbulent kinetic energy and its dissipation rate across the viscous sublayer, buffer layer and fully turbulent region.

Although the several improvements, the main weakness of the logarithmic velocity and temperature variations still unchanged. Collins and Ciofalo[9] made another modification to the approach to make it applicable when the near-wall node was placed in the buffer region, but their contribution still have the same limitation. Avelino et al [10] used asymptotic strategy to find analytical solutions for the velocity profile, turbulent energy and dissipation rate in incompressible boundary layers, and so far still the asymptotic technique included the log-law.

Many attempts by researchers tried to takes in account for pressure gradients, but none of them incorporated the development of a more wide-ranging wall function which might capture for the effects of buoyancy. One can, develop fairly simple wall function for buoyant flows by adopting improvements to the universal log-law as proposed by Petukhov and Polyakov[11]. Such wall function could not to be very accurate but it can be better than the conventional wall functions.

The Parabolic Sub-Layer approach (PSL) developed by Iacovides & Launder For buoyant flows with simple flow geometry may be used. The PSL treatment is similar to the low-Reynolds-number approach where a fine grid resolution is used in the near wall region. The main difference is that the static pressure distribution is assumed to be uniform across near-wall region; therefore, the pressure-correction algorithm is not solved in the near-wall cells. Instead, the wall normal velocity is calculated from continuity. This method gives substantial savings and has the same level accuracy as the full low-Reynolds-number formulation, but it is still having some instability for flows in complex geometries and consequently cannot be measured as general.

In the mid-1990's, some attempts were made to develop wall functions for calculating the heat transfer and fluid flow in natural convection for example, Yuan et al[12]. The researchers reported success for natural convection cases. However, the performance of their wall functions has not been tested in mixed convection flows and, unfortunately, their approach is not valid to isothermal flows. The worst part was, as in conventional wall functions, the prescription of the velocity and temperature profiles.

The aim of this work is to investigate the heat transfer rate using various wall functions in the near wall region

II. GOVERNING EQUATIONS

The governing equations are the continuity equation, the momentum equation and the energy equation as below:
The continuity equation:

$$\frac{\partial \rho}{\partial t} + \frac{\partial(\rho U_i)}{\partial x_j} = 0$$

The momentum equation:

$$\frac{\partial(\rho U_i)}{\partial t} + \frac{\partial(\rho U_i U_j)}{\partial x_j} = -\frac{\partial p}{\partial x_i} + \frac{\partial}{\partial x_j}\left[\mu\left(\frac{\partial U_i}{\partial x_j} + \frac{\partial U_j}{\partial x_i}\right) - \left(\rho \overline{u_u u_j}\right)\right] + B_i$$

The energy equation:

$$\frac{\partial(\rho T)}{\partial t} + \frac{\partial(\rho U_j T)}{\partial x_j} = \frac{\partial}{\partial x_j}\left[\frac{\mu}{Pr\frac{\partial T}{\partial x_i}\overline{u_j\theta}}[]\right]$$

➢ *Wall-Functions Approaches:*

Most commercial CFD software employs algebraic wall function formulations to take care of the effects of the thin layer close to the wall, in order to save computational time and effort. Otherwise, the near wall mesh has to be extremely fine to resolve this sublayer. In most wall-function implementations the near wall cell storage arrangement is in general as shown in figure 1.

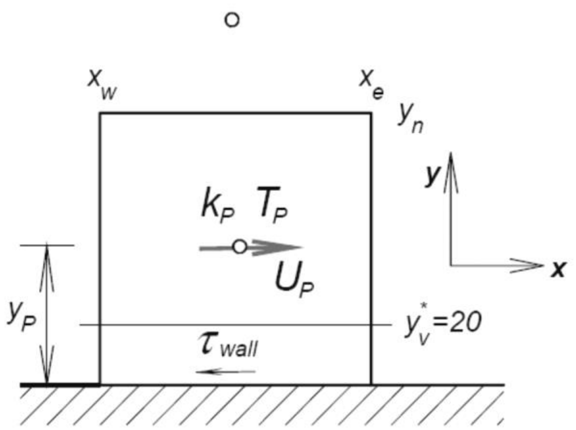

Fig 1:- Near Wall Cell Arrangement for Wall-Function

➢ *TEAM Wall-Function:*

The first assumption in the TEAM wall function is that there is a local equilibrium of turbulence energy within the thin layer close to the wall. The conventional logarithmic law is then applicable which is given by:

$$U^+ = \frac{1}{k} ln(Ey^+)$$

It is obvious that this wall-function is simple and being used with k-ε model, to calculate the wall shear stress; near wall node P is assumed and the wall shear stress is calculated at this point using the velocity as follows:

$$U^+ = \frac{U_\tau U_P}{U_\tau^2} = \frac{c_\mu^{1/4} k_P^{1/2} U_P}{\tau_{wall}/\rho} = \frac{1}{k} ln(\frac{EU_\tau y_P}{\nu})$$

Where k_P is the kinetic energy at node P, the wall shear stress is then may be obtained by:

$$\tau_{wall} = \frac{k\rho c_\mu^{1/4} k_P^{1/2} U_P}{ln\left(Ey_P\sqrt{\tau_{wall}/\rho}/\nu\right)}$$

when the wall shear stress is vanished (for example when the separation flow or reattachment point is the case), the turbulence viscosity becomes zero where in fact it has large value in the turbulent region, so the focus was on avoiding such a problem, the best choice was by replacing the wall shear stress by the turbulence energy according to Launder and Spalding [13], the new expression for the wall shear stress is then obtained by:

$$\tau_{wall} = \frac{k\rho c_\mu^{1/4} k_P^{1/2} U_P}{ln\left(Ec_\mu^{1/4} y_P^*\right)}$$

And hence the averaged production maybe expressed as:

$$\overline{P_k} = \frac{1}{y_n}\int_o^{y_n} -\rho\overline{uv}\frac{\partial U}{\partial y}\partial y = \tau_{wall}\frac{U_P}{y_P}$$

The dissipation rate is simply obtained by assuming that the shear stress is equal to the turbulent shear stress, i.e.:

$$-\rho\overline{uv} = \tau_{wall} = \mu_t\frac{\partial U}{\partial y} = \rho c_\mu \frac{k^2}{\varepsilon}\frac{\partial U}{\partial y} = \rho c_\mu \frac{k^2}{\varepsilon}\frac{U_P}{y_P}$$

Hence after using an expression for U_P to get the dissipation rate that yields:

$$\overline{\varepsilon} = \frac{c_\mu^{3/4} k_P^{3/2} U_P^+}{y_P}$$

In order to obtain the dissipation rate at the near wall node P, the next formula may be used

$$\varepsilon = \frac{k^{3/2}}{l} = \frac{k_P^{3/2}}{c_l y_P}$$

➢ *Standard Wall-Function:*

In general, the standard wall-function is similar to the TEAM wall-function. The main characteristic of this wall-function are the log-law to obtain the wall shear stress and the use of average kinetic energy production and the average dissipation rate in solving the energy equation in the near wall cells, while in the viscous sublayer the turbulent shear stress is equal to zero and the kinetic energy is assumed as:

$$k \propto y^2$$

Hence only the averaged production is changed whereas the shear stress is as the same in the Team wall-function, so the production is given by:

$$\overline{P_k} = \frac{1}{y_n}\int_{y_v}^{y_n} \frac{\tau_{wall}^2}{kc_\mu^{1/4}\rho k_P^{1/2} y}\partial y = \frac{\tau_{wall}^2}{kc_\mu^{1/4}\rho k_P^{1/2} y_n} ln\left(\frac{y_n}{y_v}\right)$$

In the same manner the averaged dissipation rate may be obtained from the following expression:

$$\overline{\varepsilon} = \frac{1}{y_n}\left[\int_0^{y_v}\frac{2\mu k_P}{\rho y_v^2}dy + \int_{y_v}^{y_n}\frac{k_P^{3/2}}{c_l y}dy\right] = \frac{1}{y_n}\left[\frac{2k_P^{3/2}}{y_v^*} + \frac{k_P^{3/2}}{c_l} ln\left(\frac{y_n}{y_v}\right)\right]$$

➢ *Chieng-Launder Wall Function:*

Unlike the standard wall function, in the Chieng-Launder wall-function the shear stress and the kinetic energy are assumed to be varies in the near wall cell as the distance from the wall increases, whereas within the viscous sub layer it is similar to the standard wall-function, The Chieng-Launder wall function has been shown to give reasonable results in the case of an abrupt pipe expansion or backward facing step, when separation occurs .the kinetic energy is given by the following expression:

$$k = k_v\left(\frac{y}{y_v}\right)$$

Where k_v is the kinetic energy at the edge of the viscous sub layer and is given by:

$$k_v = k_N - \frac{k_N - K_p}{y_N - y_P}(y_N - y_v)$$

The wall shear stress is given based on the viscous kinetic energy and is obtained from:

$$\tau_{wall} = \frac{k\rho c_\mu^{1/4} k_v^{1/2} U_P}{ln\left(E^* k_v^{1/2} y_p/\nu\right)}$$

Where $E^*$is a constant based on the viscous sub layer dimensional distance ($y_v^* = 20$)

Similarly, the energy production is expressed as:

$$\overline{P_k} = \frac{1}{y_n}\int_{y_v}^{y_n} \tau\left(\frac{\partial U}{\partial y}\right)dy$$

$$= \frac{\tau_{wall}^2}{kc_\mu^{1/4}\rho k_v^{1/2} y_n} ln\left(\frac{y_n}{y_v}\right) + \frac{\tau_{wall} - (\tau_n - \tau_{wall})}{kc_\mu^{1/4}\rho k_v^{1/2} y_n^2}(y_n - y_v)$$

Also, the average dissipation rate is given by:

$$\bar{\varepsilon} = \frac{1}{y_n}\left[\frac{2\mu k_v}{\rho y_v} + \int_{y_v}^{y_n}\frac{1}{c_l y}\left(k_n - \frac{k_n - k_P}{y_n = y_P}(y_n - y)\right)^{3/2} dy\right]$$

➤ *Johnson-Launder Wall Function:*

The main improvement in this wall function, was to modify the dimensional distance of the viscous sublayer, the reason behind this, is to take in consideration all the effects the rapid increase or decrease to the wall shear stress, they have proposed the following modification to the dimensionless thickness as:

$$y_v^* = \frac{y_{v0}^*}{1 + c\lambda}$$

Where
y_{v0}^* is the dimensionless viscous sublayer=20
C=3.1

$$\lambda = \frac{k_v - k_{wall}}{k_v}$$

The Johnson-Launder modification improved the predictions in the recirculating zone but resulted in an overestimation of the heat transfer in the downstream region, moreover it can be numerically unstable.

➤ *Thermal Wall-Function*

Wall-function based on the log law, in this approach the wall temperature can be obtained based on the boundary conditions from the expression:

$$T^* = \frac{1}{x^*} ln(E'^* y^*)$$

Where E'^* is function of molecular Prandtl number

$$x^* = xc_\mu^{1/4} = 0.25$$

Equation (3.28) may be rearranged using the hydrodynamic log-law as:

$$T^* = Pr_t\left(U^* + \frac{p}{c_\mu^{1/4}}\right)$$

Where Pr_t is the turbulent Prandtl number and the pee-function p is given by:

$$p = 9.24\left[\left(\left(\frac{Pr}{Pr_t}\right)^{0.75} - 1\right)\left[1 + 0.28\, exp\left(-0.007\frac{Pr}{Pr_t}\right)\right]\right]$$

The wall temperature can be calculated from:

$$T_{wall} = \frac{q_{wall} T^*}{\rho c_p k_p^{1/2}} + T_p$$

Where T^* is defined as:

$$T^* = \frac{\rho c_p k_p^{1/2}(T_{wall} - T)}{q_{wall}}$$

It is important to mention that the previous equation has limited applicability. For example, in natural convection flows this formula doesn't work perfectly because the logarithmic velocity and temperature profiles are not valid in such a case. Therefore, many attempts have been made to derive wall functions suitable for natural convection in order to find a better alternative to the conventional wall functions. Many researchers have based wall functions on dimensional analysis and similarity conditions for natural convective boundary layers. The disadvantages of such wall functions are that they still tend to be based on the log-law.

ISSN No:-2456-2165

The developers tuned their wall functions to one specific type of flow. One of the dimensionless temperature proposed wall functions may be obtained from the following expression:

$$T^{**} = \frac{(\rho c_p)^{3/4} (g\beta)^{1/4} (T_{wall} - T)}{q^{3/4}{}_{wall}}$$

And the dimensionless distance and temperature are given by:

$$y^{**} = \frac{y}{\alpha} \left(\frac{g\beta q_{wall}}{\rho c_p} \right)^{1/4}$$

Where:

$T^{**} = y^{**}$ For $y^{**} \leq 1$

And:

$T^{**} = 1 + 1.36\, ln\, y^{**} - 0.135\, ln(y^{**})^2$ For $1 \leq y^{**} \leq 100$

$T^{**} = 44$ For $y^{**} > 100$

➢ *Developing the Analytical Wall-Function (AWF)*

The wall shear stress and turbulent kinetic energy production and wall temperature in the conventional Wall-Functions are all based on the log law for velocity and temperature profiles. Unfortunately, these may not give accurate solutions when the flow departs from a state of local equilibrium. In this dissertation the focus is on buoyancy-influenced flow, where substantial near-wall variations of transport properties take place and where the influence of the gravitational force plays a role in modifying the shear stress profile. Conventional wall functions do not take into consideration such effects of such a flow. As a result of the above weaknesses, previous work at Manchester (Gerasimov, Craft, Launder and Iacovides[14]) developed a new wall function, named UMST-A abased on the analytical solution of the simplified Reynolds equations and which takes into account such effects as convection, pressure gradients, the influence of buoyant forces and changes in the thickness of the viscous sublayer. The full derivation equations will be skipped due to the very long terms, but can be found in Gerasimov[15].

The simplified energy and momentum Reynolds equation near the wall for forced convection can be expressed as:

$$\frac{\partial(\rho UU)}{\partial x} + \frac{\partial(\rho UV)}{\partial y} = -\frac{\partial p}{\partial x} + \frac{\partial}{\partial y}\left[(\mu + \mu_t)\frac{\partial U}{\partial y}\right]$$

$$\frac{\partial(\rho UT)}{\partial x} + \frac{\partial(\rho VT)}{\partial y} = \frac{\partial}{\partial y}\left[\left(\frac{\mu}{Pr \frac{\mu_t}{Pr_t}} () \frac{\partial T}{\partial y}\right)[]\right]$$

Where μ_t and Pr_t are the turbulent viscosity and turbulent Prandtl number respectively.

The above mentioned expressions are only in fact the transport equations with some assumptions, these assumptions may be summarised as that the pressure gradient pressure parallel to the wall is assumed to be constant across the near wall cell, another assumption; the diffusion of momentum parallel to the wall is assumed to be neglected with respect to that normal to the wall. After some manipulation, in terms of dimensionless distance from the wall y^* when the buoyancy term is exist as:

$$\frac{\partial}{\partial y^*}\left[(\mu + \mu_t)\frac{\partial U}{\partial y^*}\right] = C + b(T - T_{ref})$$

$$\frac{\partial}{\partial y^*}\left[\left(\frac{\mu}{Pr \frac{\mu_t}{Pr_t}} () \frac{\partial T}{\partial y^*}\right)[] \frac{\mu_v^2}{\rho_v^2 k_p}\left(\rho U \frac{\partial T}{\partial x} + \rho V \frac{\partial T}{\partial y}\right)_{th}\right]$$

where:

$$C = \frac{\mu_v^2}{\rho_v^2 k_p}\left[\rho U \frac{\partial U}{\partial x} + \rho V \frac{\partial V}{\partial x} + \frac{\partial P}{\partial x}\right]$$

$$b = -\frac{\mu_v^2}{\rho_v^2 k_p} \rho_{ref}\, g\beta$$

To solve this equation for the temperature, it is assumed that only the first term in non-conservative is considered, i.e,

$$C_{th} = \frac{\mu_v^2}{\rho_v^2 k_p} \rho U \frac{\partial T}{\partial x}$$

By integrating separately over the viscous and turbulent regions of the near-wall cell by assuming C_{th} is constant across the sublayer with continuity of T and $\left.\frac{\partial T}{\partial y^*}\right|_{y=y_v}$, the result can be written as:

$$T = \begin{cases} T_{wall} + \dfrac{Pr}{\mu_v \left[\frac{C_{tn} y^{*2}}{2} + A_{th} y^*\right]_v^{**}} \\ T_{wall} + \dfrac{Pr}{\mu_v \alpha_{t\,th}(y^* - y_v^*)} \\ + \dfrac{Pr}{\mu_v \alpha_t \left[A_{th} + C_{th}\left(y_v^* - \frac{1}{\alpha_t}\right)\right] ln\, Y_T} \\ + \dfrac{Pr\, y_v^*}{\mu_v}\left[\dfrac{C_{tn} y^*}{2} + A_{th}\right], y^* > y_v^* \{ \end{cases}$$

where:

$$\alpha_t \equiv \frac{Pr\, \alpha}{Pr_t}$$

$$Y_T \equiv [1 + \alpha_t(y^* - y_v^*)]$$

$$A_{th} \equiv -\frac{q_{wall} \mu_v}{c_p \rho_v \sqrt{k_p}}$$

The integration may be obtained separately by assuming C as constant across the viscous sublayer and the fully turbulent region where:

$$\mu_t = 0 For y^* < y_v^*$$
$$\mu_t = \mu\alpha(y^* - y_v^*) For y^* > y_v^*$$

Hence:

$$\frac{\partial}{\partial y^*}\left[\mu\frac{\partial U}{\partial y_*}\right] = C_1$$

Where

$$C_1 = \frac{\mu_v^2}{\rho_v^2 k_p}\left[\rho U_P\frac{(U_e - U_w)}{\Delta x_{ew}} + \frac{\partial P}{\partial x}\right]$$

The result is that the wall shear stress can be obtained from:

$$\tau_{wall} = -\frac{\rho\sqrt{k_P}}{\mu}A_1$$

Where

$$A_1 = \frac{\mu_v U_n - N}{\left[\frac{ln\, Y_n}{\alpha} + y_v^*\right]}$$

U_n is interpolated using nodal values U_P and U_N

and

$$N = \frac{C_2}{\alpha}\left[y_n^* - \left(\frac{1}{\alpha} - y_v^*\right)ln\, Y_n\right] + \frac{C_1 - C_2}{\alpha}y_v^*\, ln\, Y_n + \left(\frac{C_1}{2}y_v^* - \frac{C_2}{\alpha}\right)y_v^*$$

The cell averaged turbulent kinetic energy production is given by:

$$\overline{P_k} = \frac{1}{y_n}\frac{\rho_v\sqrt{k_p}}{\mu_v}\int_{y_v^*}^{y_n^*}\mu_v\alpha(y^* - y_v^*)\left(\frac{\partial U_2}{\partial y^*}\right)^2 dy^*$$

where

$$\frac{\partial U_2}{\partial y^*} = \frac{1}{\mu_v Y}\left[Cy^* + A_2 + b\left(T_v - T_{ref} + \delta T_y y_v^*\right)y^* - b\frac{\delta T_y y_v^{*^2}}{2}\right]$$

and

$$A_2 = b y_v^*\left[\frac{T_{wall} - T_v}{2} - \frac{T_v - T_n}{y_n^* - y_v^*}\frac{y_v^*}{2}\right] + A_1$$

The expression of the velocity within the viscous sublayer obtained from the integration of the momentum equation and give by:

$$\mu_v U_1 = \frac{C}{2}y^{*^2} + A_1 y^* + \frac{b}{2}\left(T_{wall} - T_{ref}\right)y^{*^2} - \frac{b}{6y_v^*}\left(T_{wall} - T_v\right)y^{*^3} + bb_\mu y^{*^2}\left(T_{wall} - T_{ref}\right) \times \left(\frac{y^*}{3} - \frac{y_v^*}{2}\right) - \frac{bb_\mu y^{*^3}}{2y_v^*} \times \left(T_{wall} - T_v\right)\left(\frac{y^*}{4} - \frac{y_v^*}{3}\right) + b_\mu C y^{*^2}\left(\frac{y^*}{3} - \frac{y_v^*}{2}\right) + b_\mu A_1 y^*\left(\frac{y^*}{2} - y_v^*\right)$$

Whereas in the fully turbulent region ($y^* > y_v^*$), the expression takes form:

$$\mu_v U_2 = \frac{C}{\alpha}\left[y^* - \left(\frac{1}{\alpha} - y_v^*\right)ln\, Y\right] + \frac{A_2}{\alpha}ln\, Y + b\frac{\left(T_v - T_{ref} + \delta T_y y_v^*\right)}{\alpha} \times \left[y^* - \left(\frac{1}{\alpha} - y_v^*\right)ln\, Y\right] - b\frac{\delta T_y}{2\alpha}\left[\frac{y^{*^2}}{2} - y^*\left(\frac{1}{\alpha} - y_v^*\right) + \left(\frac{1}{\alpha} - y_v^*\right)^2 ln\, Y\right] + B2$$

The cell averaged buoyant source term in the momentum equation can be found from:

$$\overline{F_b} = \beta'\left[\left(\frac{T_{wall} + T_v}{2} - T_{ref}\right)y_v^* + \left(\frac{T_v + T_n}{2} - T_{ref}\right)(y_n^* - y_v^*)\right]$$

where

$$\beta' = \frac{\rho_{ref}\, g\beta\mu_v}{y_n\rho_v\sqrt{k_P}}$$

The cell averaged dissipation rate is given by integration over the wall control volume:

$$\bar{\varepsilon} = \frac{1}{y_n}\left[\frac{2k_p^{3/2}}{y_d^2} + \frac{k_p^{3/2}}{2.55}ln\left(\frac{y_n}{y_d}\right)\right]$$

which is as shown in figure (2)

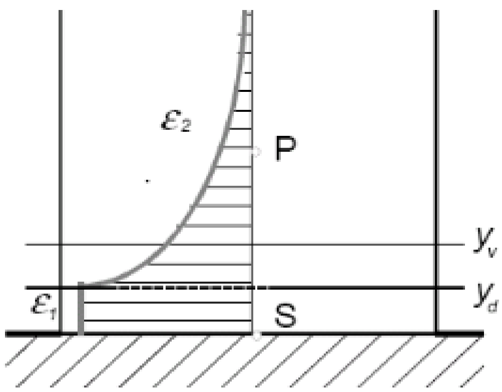

Fig 2:- Dissipation Rate Distribution

It was established by Gerasimov[15] that the cell averaged dissipation rate needed to be modified by a scaling function $F_\varepsilon$to cope with the variation in the viscous sublayer region, the modified average dissipation rate is expressed as:

$$\bar{\varepsilon}_{new} = F_\varepsilon \bar{\varepsilon}_{old}$$

The scaling function proposed by hem is given by:

$$F_\varepsilon = \begin{cases} 1 + 1.5\{1 - exp[-6.9(\lambda - 0.98)]\} for \lambda \geq 1.0 \\ \times \{1 - exp[-193(max(\alpha, 0))^2]\}, \\ 1 - (1 - F_{\varepsilon 0}) \left[1 - exp\left(-\frac{1-\lambda}{\lambda}\right)\right] \\ \times \{1 - exp[-11.1(max(\gamma, 0))^2]\} for \lambda < 1.0 \end{cases}$$

where
$F_{\varepsilon 0}$=0.75

$$\lambda = \frac{\mu_w \sqrt{\left(\frac{\partial U_i}{\partial x_j}\right)_w \left(\frac{\partial U_i}{\partial x_j}\right)_w}}{\mu_v \sqrt{\left(\frac{\partial U_i}{\partial x_j}\right)_v \left(\frac{\partial U_i}{\partial x_j}\right)_v}}$$

$$\alpha = \frac{\lambda}{1.02} - 1$$

Sine Gerasimov[15] modelled the effect of accelerating or decelerating of buffer layer by introducing a factor by which he multiplied the cell averaged dissipation rate, and that after testing a number of alternatives he based this function on the ratio of the wall shear stress to the shear stress at the edge of the viscous sublayer. This scaling function was not total in separated or reattachment flows, subsequent work by Gulguzel found that in such cases it did not perform well, he tested a number of alternatives in separated flows, the form he proposed adopting is, the present work include applying this form to the type of flows that Gerasimov studied to see if it performs as well as the original version The reason behind introducing this new scaling function is that despite the good results obtained in free flow, the approach has failed in other types of flow such as separation or reattachment flows, the new scaling function is simply expressed as:

$$F_\varepsilon = \begin{cases} 1 if C_o \leq 0 \\ -28.333 C_o + 1 if 0 < C_o \leq 0.03 \\ 0.15 if C_o > 0.03 \end{cases}$$

Where C_o is the non dimensional of the convective term in the momentum equation, the non-dimensional form of the convective term is obtained using the Kolmogorov scales as:

$$C_o = \frac{C(c_l y_P)^{3/4}}{k_P^{1/8} \nu^{7/4} \rho}$$

where C is

$$C = \frac{\mu_v^2}{\rho_v^2 k_p}\left[\rho U \frac{\partial U}{\partial x} + \rho V \frac{\partial V}{\partial x} + \frac{\partial P}{\partial x} - g(\rho - \rho_{reff}\right]$$

The scaling function form was arrived by determining the value of F_ε that is needed to give very close agreement with the low-Reynolds number predictions of the k-ε model for mixed and forced convection in a pipe.

III. RESULTS AND DISCUSSION

The governing equations were solved with boundary conditions with constant inlet velocity and zero outlet pressure gauge with an external constant heat flux. The results for different wall functions were presented and analysed.

The variation of the near wall temperature at the vertical wall for four wall functions is presented in Figure 3. The temperature decreased with the increase in the hight of the pipe. It was found that the enhanced wall function showed a higher temperature distribution.

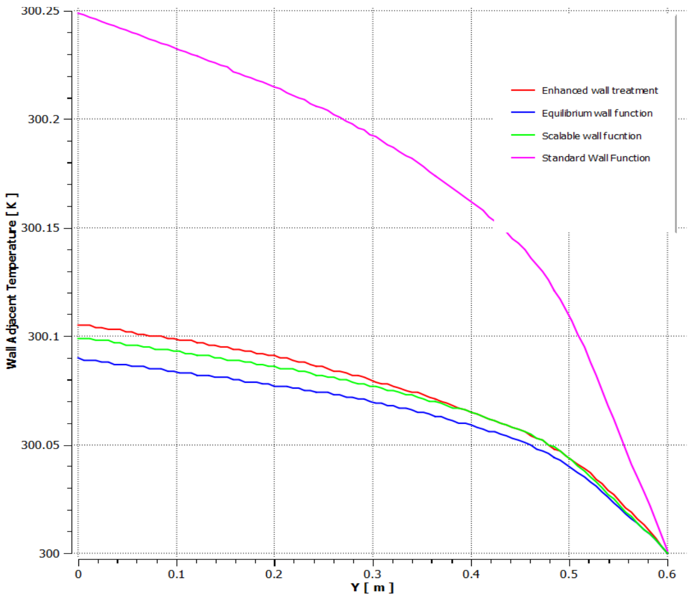

Fig 3:- Variation of Wall Temperature for Various Wall Functions

The wall function techniques have also an effect on the turbulent kinetic energy, the variation of the Turbulent energy on the wall for several wall functions tested as shown in Figure 4. The turbulent kinetic energy dropped significantly at the inlet of the pipe. It can be clearly seen the equilibrium wall function showed the least performance in capturing the turbulent kinetic energy among different wall functions

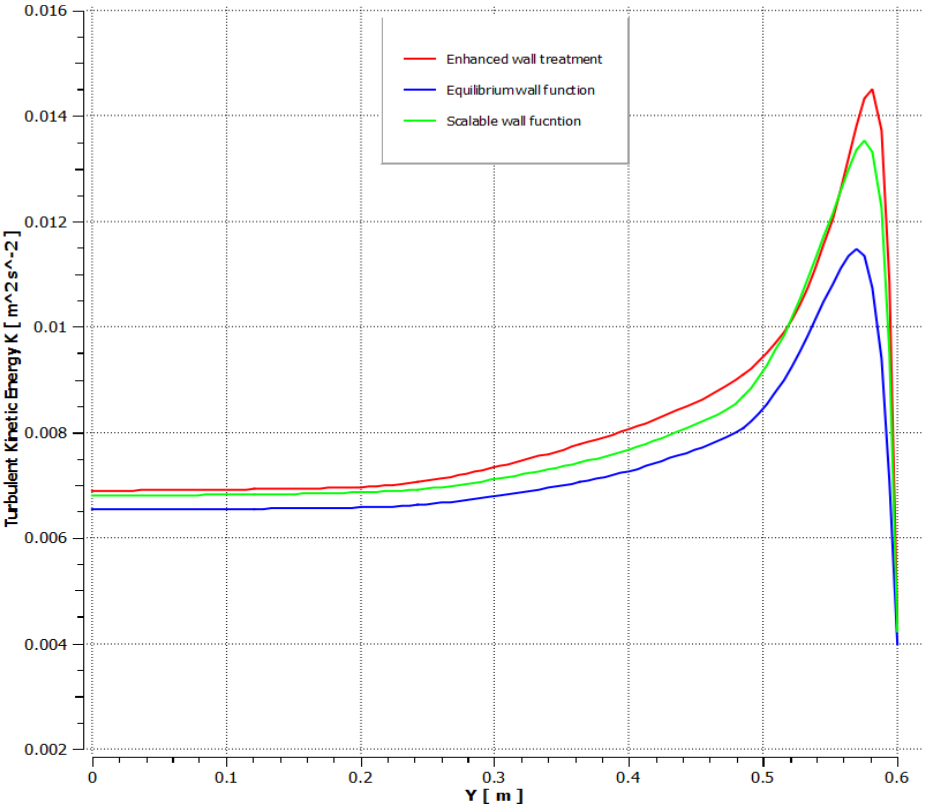

Fig 4:- The Variation of the Turbulent Energy on the Wall for Several Wall Functions

The temperature distribution on a vertical line in the core of the cylinder was also investigated and the results are depicted in Figure 5, It is evident that the standard wall function over-estimated the temperature in this location, this is attributed to the assumption of averaged kinetic production out of the viscous sublayer.

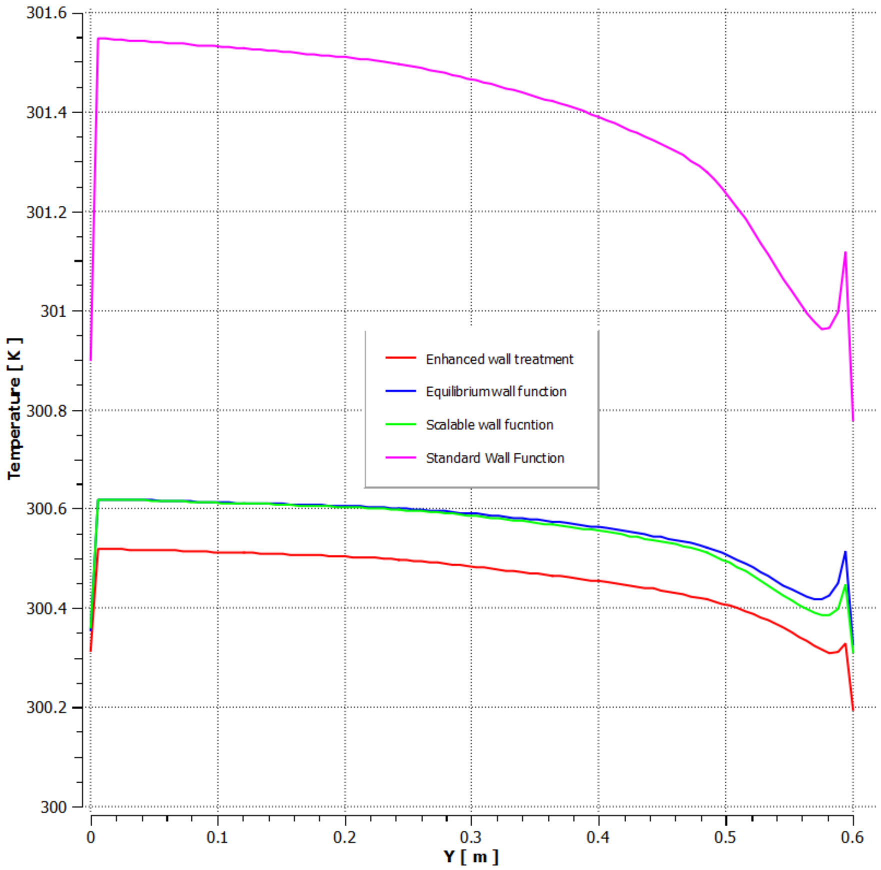

Fig 5:- The Temperature Distribution on the Center Line of the Cylinder

To give a better understanding to turbulence dissipation using several wall functions, the turbulence dissipation rate on the wall employing different wall functions was examined and the results are illustrated in Figure 6. The turbulence showed a sharp growth at the entrance of the pipe and dropped significantly with the advance of the flow in the pipe, it is worth to mention that the enhanced wall function showed a better estimation of the turbulence eddy dissipation rate over the other two functions.

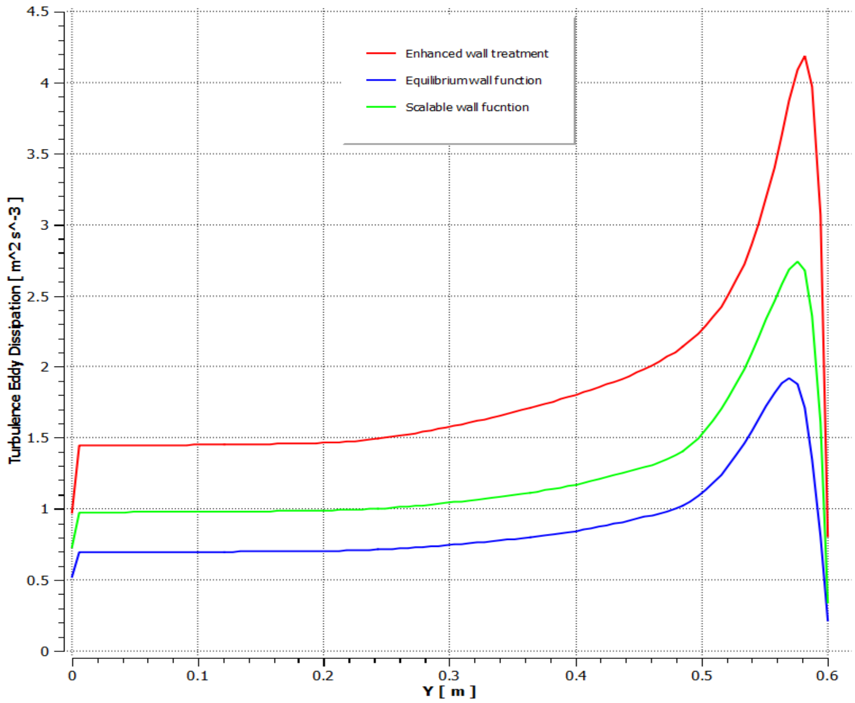

Fig 6:- Turbulence Dissipation Rate on the Wall for Different Wall Functions

The pressure coefficient on the wall was also investigated and the results are shown in Figure 7, the pressure coefficient reduced sharply at the entrance and decreased gradually away from the entrance, all wall functions showed similar prediction for pressure coefficient, however, enhanced wall function gave 5% higher than other wall functions

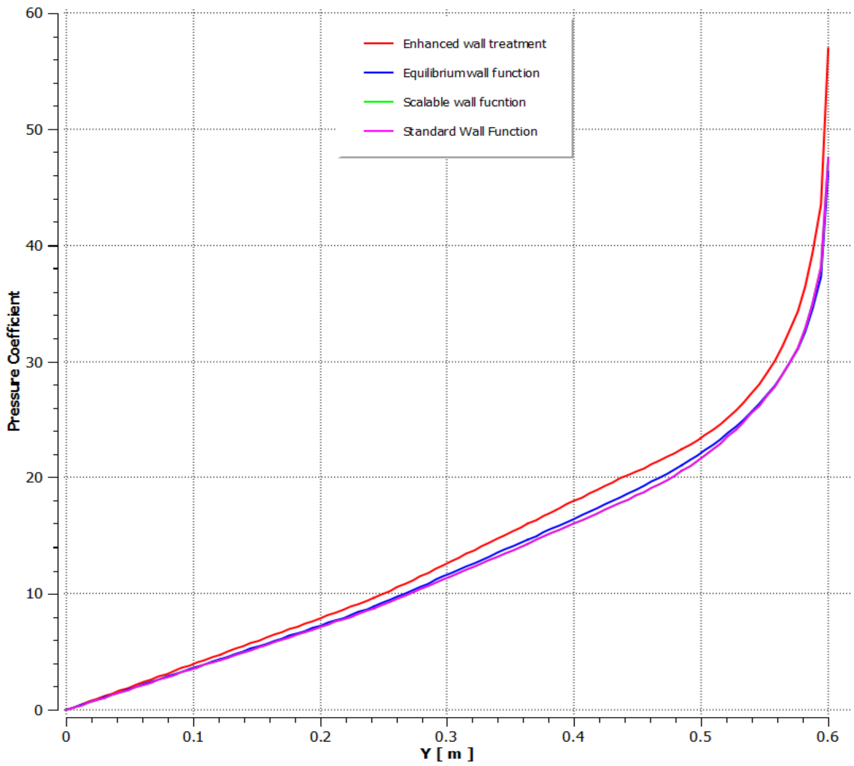

Fig 7:- The Variation of Pressure Coefficient on the Wall

To examine the heat transfer performance in the near wall region, the applicability of all functions was tested and the results are presented in Figure 8. The graph shown displays the variation of Nu number which gives an indication to the heat transfer rate along the pipe wall. It can be clearly seen that the enhanced wall function showed the best prediction for Nu number over the other two wall functions.

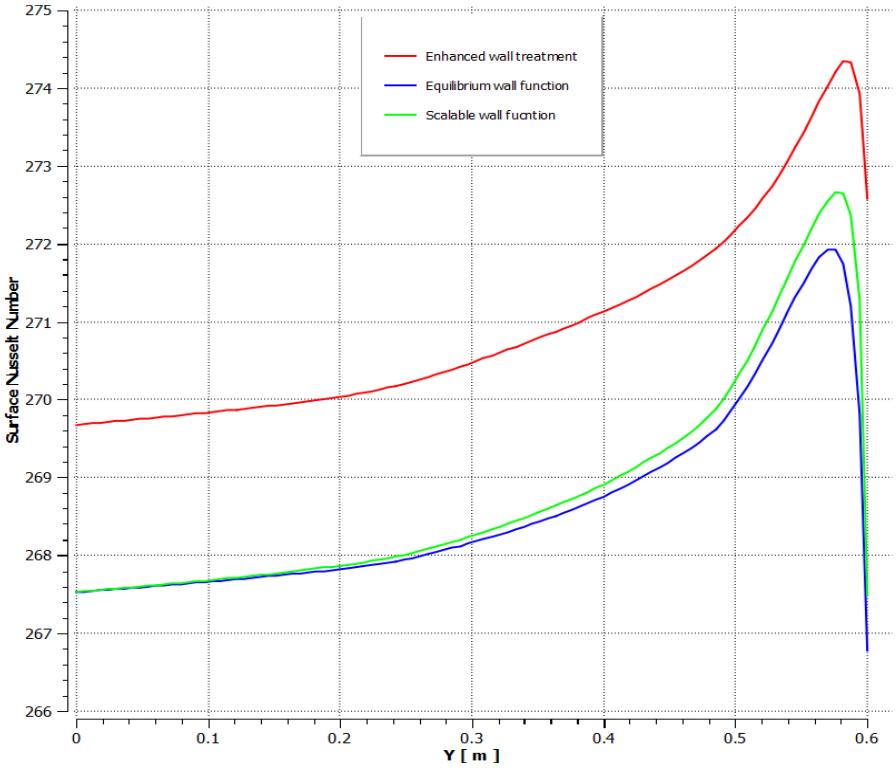

Fig 8:- Variation of Nu number at wall for different wall function.

The turbulent energy variation on the wall of the pipe is investigated. The results are demonstrated in Figure 9. It was found that the equilibrium wall function prediction was the worst at both the entry region and at along the pipe. However, when the departed the entry region, the production behaviour remains unchanged for all wall functions.

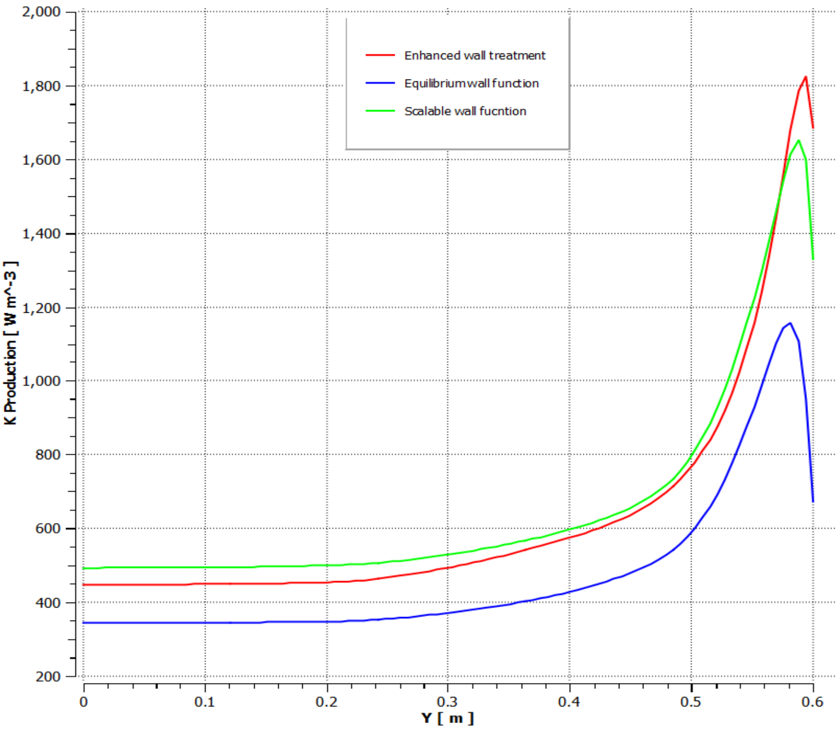

Fig 9:- Variation of Production along the Wall

The turbulent energy variation on the centre line of the pipe is investigated. The results are demonstrated in Figure 10. It was found that the enhanced wall function prediction was the highest at the entry region. However, when the flow departed the entry region, the production dropped significantly and it was almost the same prediction by all wall functions.

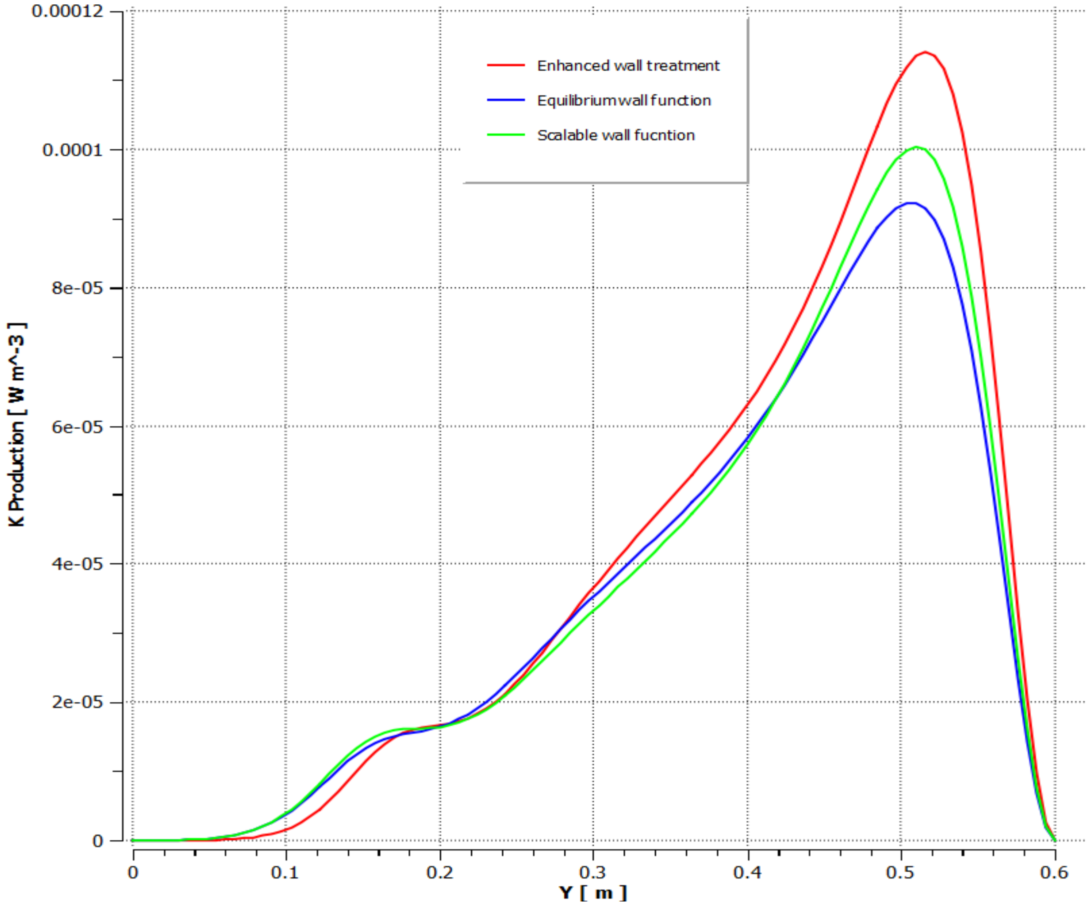

Fig 10:- The Turbulent Energy Variation on the Center Line of the Pipe

IV. CONCLUSION

The heat transfer rate in the very near wall region was studied using various wall functions in a vertical pipe with constant heat flux, four wall functions were tested and the results were shown and discussed. The enhanced wall function showed a better prediction among all functions tested. The wall functions strategy is essential for the CFD computational cost to minimise the simulation cost. Despite the fairly well applicability of the enhanced wall function, further work is needed to improve its applicability for complex types of flows.

REFERENCES

[1]. Craft, T.J., et al., *Progress in the Generalization of Wall-Function Treatments.* International Journal of Heat and Fluid Flow, 2002. **23**: p. 148.

[2]. SPALDING, D.B., *Monograph on turbulent boundary layers*. 1967, Imperial College, Dept. of Mech.Eng.

[3]. Spalding., D.B., *Monograph on turbulent boundary layers*, . Department of Mechanical Engineering, Imperial College of Science and Technology,, 1967. **Chapter 2. Technical Report TWF/TN/33,**.

[4]. M.Wolfshtein., *The velocity and temperature distribution in one-dimensional flow with turbulence augmentation and pressure gradient.* . International Journal of Heat and Mass Transfer, 1969. **12**: p. 301—318.

[5]. Chieng, C.C.a.B.E.L., *On the calculation of turbulent heat transfer downstream from an abrupt pipe expansion.* . Numerical Heat Transfer., 1980. **3**: p. 189—207.

[6]. Johnson, R.W. and B.E. Launder, *On the calculation of turbulent heat transfer downstream from an abrupt pipe expansion.* Numerical Heat Transfer, 1982. **5**: p. 493—496.

[7]. Amano, R.S., *A study of turbulent flow downstream of an abrupt pipe expansion.* AIAA Journal,, 1983. **21(10)**: p. 1400—1405.

[8]. Amano, R.S., *Development of a turbulence near-wall model and its application to separated and reattached flows.* Numerical Heat Transfer,, 1984. **7**: p. 59-75.

[9]. Ciofalo, M. and M.W. Collins, *k-*. International journal of Heat Mass Transfer, 1989. **15**: p. 21-47.

[10]. Avelino, M.R.J. and A.P.S. Freire, *An analytical near wall solution for the k-ε model for transpired boundary layer flows.* . International Journal of Heat and Mass Transfer, 1999. **42**: p. 3085—3096.

[11]. Petukhov, B.S., et al., *EXPERIMENTAL STUDY OF HEAT TRANSFER IN PIPES WITH VARIABLE DENSITY OF THE HEAT FLUX THROUGH THE WALL.* Heat Transfer Sov Res, 1977. **9**(4): p. 114-122.

[12]. Yuan, X., A. Moser, and P. Sutter, *Application of new wall functions in prediction of turbulent natural convection. International Symposium on Turbulence.* International Symposium on Turbulence, Heat and Mass Transfer, Lisbon, August 1994.

[13]. Chieng, C.-C. and B. Launder, *On the calculation of turbulent heat transport downstream from an abrupt pipe expansion.* Numerical Heat Transfer, 1980. **3**(2): p. 189-207.

[14]. Craft, T.J., et al., *Development and Application of Wall-Function Treatments for Turbulent Forced and Mixed Convection Flow.* Fluid Dynamics Research, 2006. **38**: p. 127.

[15]. Gerasimov, A.V., *Development and validation of an analytical wall-function strategy for modelling forced, mixed and natural convection flows* 2004, Mnchester umist.